DOI: 10.1002/ejic.200900205

Competing Large and Small Angles in a Double End-On Azido Copper(II) Binuclear Complex: A Combined Experimental and Theoretical Study of Magnetic Interactions

Qin-Xiang Jia,[a] Marie-Laure Bonnet,[b] En-Qing Gao,*[a] and Vincent Robert*[b]

Keywords: Ab initio calculations / Azides / Copper / Density functional calculations / Magnetic properties

The structure and magnetic properties of double azido-bridged Cu^{II} binuclear complex **1** with the chelating chiral ligand (*S*,*S*)-2,2′-isopropylidenebis(4-phenyl-2-oxazoline) were analyzed by combining experimental and theoretical techniques. The Cu^{II} ions adopt a square pyramidal geometry with different degrees of distortion, whereas the two end-on azido bridges disposed at the equatorial positions exhibit significantly different Cu–N–Cu angles, 110.6 and 97.3°, which are respectively smaller and larger than the critical 108° value distinguishing the ferromagnetic and antiferromagnetic regimes. The asymmetry in **1** arises from the use of the bulky asymmetric ligand, giving rise to two different magnetic pathways between the Cu^{II} ions. The magnetic pathway along the large Cu–N–Cu angle value dominates over the small one, resulting in a net antiferromagnetic behavior with $J = -78.6$ cm^{-1}. On the basis of wavefunction calculations, we investigate the exchange interactions in synthetic compound **1** and fictitious analogs **2** and **3** holding either two large (i.e., 110.6°) or two small (i.e., 97.3°) Cu–N–Cu angles. The calculated exchange interaction in **1** (–104 cm^{-1}) is in relatively good agreement with the experimental value and corresponds precisely to the average between the antiferromagnetic value in **2** (–218 cm^{-1}) and the ferromagnetic one in **3** (21 cm^{-1}). The significant enhancement in the antiferromagnetic contribution accompanying the expansion of one of the Cu–N–Cu bridging angles is undoubtedly the driving force for the observed antiferromagnetic behavior in **1**. The control of the local metal environments allowed us to monitor the exchange coupling interactions.

Introduction

Molecular magnetism of polynuclear complexes, in which paramagnetic metal ions are connected by small bridges to form discrete or extended structures, has been an active field of research for decades.[1] Among the large variety of bridging ligands used, the azido ion has attracted considerable attention for its versatility and efficiency in bridging metal ions and mediating magnetic exchange.[2] As a matter of fact, numerous azido-bridged metal compounds with various structural topologies and magnetic properties have been reported.[2–5] Nevertheless, simple model systems are still desirable for the purpose of better understanding the magnetic exchange mechanism and obtaining magnetostructural correlations. In this context, particular attention has been paid to binuclear azido-bridged Cu^{II} systems,[6–11] which have a limited number of electrons (i.e., two unpaired electrons) involved in the interaction and provide the simplest model. Cu^{II} ions usually adopt either a square planar, square pyramidal, or axially elongated octahedral geometries and are bridged by two azido ions in the μ-1,1 (end-on, EO)[6–9] or μ-1,3 (end-to-end, EE)[4a,4b,10,11] modes (Scheme 1). The bridge may adopt the "symmetric" equatorial–equatorial (eq–eq) fashion (i.e., occupy the equatorial positions of both Cu ions; Scheme 1c), with two comparable short Cu–N bonds (1.97–2.14 Å),[6,7,10] or the asymmetric equatorial–axial (eq–ax) fashion (i.e., occupy the equatorial position of one Cu ion but the axial position of the other metal ion; Scheme 1d) with short (1.97–2.08 Å, equatorial) and long (2.19–2.85 Å, axial) Cu–N bonds.[8,9,11] It is now accepted that the nature and magnitude of the magnetic exchange are not only dependent upon the bridging mode (EO or EE), but also strongly influenced by the arrangement (eq–eq or eq–ax) of the azido bridge between the metal ions.

The observation that the EO azido bridge can transmit strong ferromagnetic interactions, which are more relevant to the design of molecular magnets than antiferromagnetic ones, has evoked extensive experimental and theoretical studies.[6,7,12–15] Earlier studies seemed to suggest that the

[a] Shanghai Key Laboratory of Green Chemistry and Chemical Processes, Department of Chemistry, East China Normal University,
Shanghai 200062, China
Fax: +86-21-62233404
E-mail: eqgao@chem.ecnu.edu.cn
[b] Université de Lyon, Ecole normale supérieure de Lyon and CNRS, Laboratoire de Chimie,
46 allée d'Italie, 69364 Lyon cedex 07, France
E-mail: vincent.robert@ens-lyon.fr

Supporting information for this article is available on the WWW under http://dx.doi.org/10.1002/ejic.200900205.

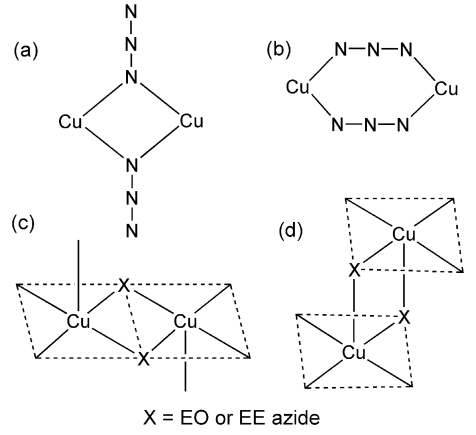

Scheme 1. The end-on (EO, a) and end-to-end (EE, b) coordination modes and the equatorial–equatorial (eq–eq, c) and equatorial–axial (eq–ax, d) disposition fashions of the azido bridge.

EO azido bridge mediates intrinsic ferromagnetic exchange through a spin polarization mechanism.[6b,12] Nevertheless, such a picture was reconsidered. An increasing number of Cu^{II} compounds with eq–ax EO azido bridges have been reported with magnetic interactions ranging from weak ferromagnetic to weak antiferromagnetic (J ranging from –9 to 13 cm^{-1}),[8,9] but no unambiguous magnetostructural correlation has been proposed. For systems with symmetric eq–eq EO azido bridges, experimental studies have suggested that small Cu–N–Cu bridging angle values favor the ferromagnetic behavior. Conversely, antiferromagnetism can be anticipated as soon as this angle is larger than a critical value estimated to be about 108°.[13] The angular dependence is consistent with the spin delocalization mechanism, supported by a polarized neutron diffraction study[14] and theoretical DFT calculations.[15] The small-angle ferromagnetic regime was confirmed in a number of binuclear systems with double EO azido bridges (J ranging from 23 to 230 cm^{-1}).[6,7] In contrast, the antiferromagnetic interaction for larger bridging angles has only been attributed in some mixed bridged systems, in which the metal ions are simultaneously linked by EO azido groups and bridges of other types.[13] To the best of our knowledge, synthetic species holding two large-angle eq–eq EO azido bridges have not been reported so far, nor have the species with simultaneous small- and large-angle bridges. Such systems would be highly desirable not only from the viewpoints of magnetostructural studies but also in the preparation of molecular systems with specific and controlled magnetic behavior.

In the course of our work on metal–azide systems,[4,5,9c] we obtained a unique binuclear Cu^{II} complex $[Cu_2(L)_2(N_3)_4]\cdot 0.5CH_3OH$ (**1**) with double eq–eq EO azido bridges [L = (*S*,*S*)-2,2′-isopropylidenebis(4-phenyl-2-oxazoline), Scheme 2]. The system was characterized by using X-ray diffraction and temperature-dependent magnetic susceptibility measurements. The complex is unique, because one Cu–N–Cu angle (110.6°) is larger than the critical angle value, whereas the other one is smaller (97.3°). In addition, the small-angle bridge is asymmetric with short and long Cu–N distances (2.02 and 2.32 Å), which is rather unusual for eq–eq bridges. Thus, **1** looks like a very intriguing model system to further investigate the exchange interactions through the azido magnetic couplers. Experimental studies reveal overall antiferromagnetic coupling between the Cu^{II} ions. In order to clarify the origin of the magnetic coupling and to gain magnetostructural information about the two competing pathways, quantum chemical calculations were performed on this peculiar compound. The exchange interactions were compared with those calculated for the fictitious systems with either two large (compound **2**) or two small (compound **3**) Cu–N–Cu angles. Our calculations suggest that (i) the large- and small-angle pathways mediate antiferro- and ferromagnetic exchange contributions, respectively, and (ii) the former overtakes the latter to result in a net antiferromagnetic behavior in synthetic compound **1**.

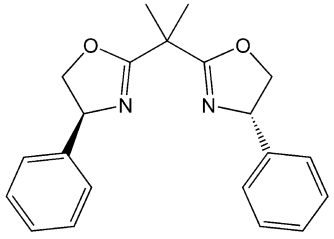

Scheme 2. The bis(oxazoline) ligand (L) used in the preparation of **1**.

Results and Discussion

Crystal Structures

According to X-ray crystallographic analyses, the structure consists of binuclear molecules in which the Cu^{II} ions are bridged by double azido ligands in the EO mode. The molecular structure is shown in Figure 1 and selected bond lengths and angles are listed in Table 1.

Both Cu^{II} ions exhibit a square-pyramidal geometry with different degrees of distortion, as clearly shown in Figure 1. For Cu1, the basal plane is formed by three azido nitrogen atoms (N8, N11 and N5) and an oxazoline nitrogen atom (N1) from the chelating organic ligand, and the axial position is occupied by the other nitrogen atom (N2) from the chelating ligand. The four basal nitrogen atoms are almost coplanar, with their deviations from the least-square plane being smaller than 0.061(4) Å. The Cu1 atom is displaced out of the basal plane by 0.252(4) Å towards the pyramidal apex. The Cu2 environment is similar, with three azido nitrogen atoms and an oxazoline nitrogen atom (N3, N5, N8, and N14) in the basal plane and another oxazoline nitrogen atom (N4) at the axial position. However, the basal plane of Cu2 is significantly distorted towards tetrahedral geometry with deviations of the basal donor atoms from the least-squares plane being in the range of 0.209(4)–0.251(4) Å. The displacement of Cu2 out of the basal plane is also

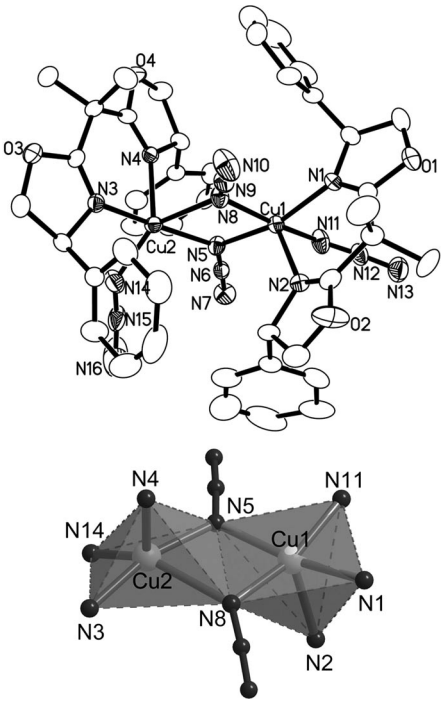

Figure 1. A perspective view of the binuclear molecule in **1** (top; hydrogen atoms are omitted and carbon atoms are not labeled for clarity) and a highlighting view of the coordination polyhedrons (bottom).

Table 1. Selected bond lengths [Å] and angles [°] in compound **1**.

Cu1–N1	2.015(6)	Cu2–N3	1.986(7)
Cu1–N2	2.181(6)	Cu2–N4	2.070(6)
Cu1–N11	1.987(7)	Cu2–N14	1.918(7)
Cu1–N5	2.013(7)	Cu2–N5	1.957(7)
Cu1–N8	2.021(7)	Cu2–N8	2.319(7)
N11–Cu1–N5	92.5(3)	N14–Cu2–N5	96.4(3)
N11–Cu1–N1	88.3(3)	N14–Cu2–N3	90.2(3)
N5–Cu1–N1	162.1(3)	N5–Cu2–N3	166.2(3)
N11–Cu1–N8	166.9(3)	N14–Cu2–N4	124.8(3)
N5–Cu1–N8	78.9(3)	N5–Cu2–N4	97.7(3)
N1–Cu1–N8	96.8(3)	N3–Cu2–N4	88.4(2)
N11–Cu1–N2	99.2(3)	N14–Cu2–N8	144.7(3)
N5–Cu1–N2	111.7(3)	N5–Cu2–N8	73.1(3)
N1–Cu1–N2	85.7(3)	N3–Cu2–N8	94.5(3)
N8–Cu1–N2	93.2(3)	N4–Cu2–N8	90.4(3)
Cu1–N8–Cu2	97.3(3)	Cu2–N5–Cu1	110.6(3)
N7–N6–N5	176.8(9)	N10–N9–N8	176.4(11)
N11–N12–N13	174.4(11)	N14–N15–N16	169.2(10)

larger [0.390(4) Å]. These parameters suggest that the geometry of Cu2 is more severely distorted than that of Cu1. According to Addison et al.,[16] the distortion of the square pyramidal geometry towards trigonal bipyramidal can be described with the geometric parameter $\tau = |\beta - \alpha|/60$, where β and α are the bond angles involving the *trans* donor atoms in the basal plane. The parameter is 0 for an ideal square pyramid and 1 for an ideal trigonal bipyramid. The calculated τ values for Cu1 and Cu2 are 0.08 and 0.358, respectively. The large value for the Cu2 ion suggests a high distortion of the coordination geometry towards trigonal bipyramidal, with two azido nitrogen atoms (N3 and N5) at axial positions.

In addition, the geometry around Cu2 exhibits an unusual feature. The square-pyramidal coordination for Cu^{II} ions usually shows axial elongation due to the Jahn–Teller effect. This is the case for Cu1, which has a long axial Cu1–N2 bond [2.181(6) Å] and four short equatorial Cu–N bonds [1.987(7)–2.021(7) Å]. In contrast, the Cu2 environment exhibits a short axial Cu2–N4 distance [2.070(6) Å], three short equatorial distances [1.918(7)–1.986(7)], and a long equatorial Cu2–N8 distance [2.319(7) Å]. At first glance, the long Cu2–N8 distance may lead to the impression that the N8 atom is at the axial position of the square pyramid. However, this assumption is not consistent with the N–Cu2–N angle data. Indeed, all the N4–Cu2–N angles are closer to 90° than to 180° (see Table 1), suggesting that N4 occupies the axial position of the square pyramid, and consistently, the N8–Cu2–N14 angle is closer to 180° than to 90°, suggesting a quasiequatorial position for N8. The quasiequatorial, instead of axial, arrangement of N8 is clearly depicted in Figure 1 (bottom). This unusual observation may be due to the steric hindrance imposed by the very bulky ligand and should have important magnetic relevance.

All the azido ions, including the bridging and terminal ones, are quasilinear with N–N–N angles in the range of 169.2(10)–176.8(9)°. The Cu1 and Cu2 atoms are connected through two nonequivalent EO azido bridges with d(Cu···Cu) = 3.265(1) Å, and both azido bridges are disposed between the two Cu^{II} ions in an eq–eq fashion, that is, the bridging nitrogen atoms lie in the equatorial planes of the Cu ions. The bridging angles of Cu1–N5–Cu2 and Cu1–N8–Cu2 are 110.6(3) and 97.3(3)°, respectively. The smaller bridging angle is associated with the long Cu2–N8 distance. The $[Cu_2N_2]$ four-membered ring is almost planar with deviations smaller than 0.007(3) Å.

To summarize, the N5 azido ion is a symmetric eq–eq bridge with short Cu–N distances and a large bridging angle, whereas the N8 azido ion is an asymmetric eq–eq bridge with short and long Cu–N distances and a small bridging angle. These particular features give rise to a quite asymmetric $[Cu_2(N_3)_2]$ bridging moiety. In the previously reported Cu^{II} dimers with the double EO azido bridges, the $[Cu_2(N_3)_2]$ moieties are usually symmetric or quasisymmetric with two comparable bridging angles.[6–7] The asymmetry in **1** arises from the use of the asymmetric ligand, which does not allow inversion and mirror symmetry in the structure. The large steric hindrance introduced by the bulky ligand may also contribute to the large discrepancies in bridging angles and bond lengths.

The binuclear molecules are isolated by the ligands and the shortest intermolecular Cu···Cu distance is 6.6 Å. Only weak hydrogen bonds are operative between neighboring molecules. Along the crystallographic *ab* plane, the molecules are associated through two independent sets of C–H···π interactions involving phenyl C–H groups and phenyl rings, and along the *c* direction, C–H···N hydrogen bonds

involving methyl groups and terminal azido nitrogen atoms are operative between neighboring molecules (see the Supporting Information).

Magnetic Properties

The magnetic susceptibility of complex **1** was measured in the 2–300 K temperature range and is shown as χT and χ vs. T plots in Figure 2. The measured χT value at 300 K is about 0.77 emu mol^{-1} K per dimer, comparable to the spin-only value of 0.75 emu mol^{-1} K for two uncoupled S = 1/2 spins. Upon cooling, while the χT value decreased monotonically, the χ value increased to a round maximum of 5.9×10^{-3} emu mol^{-1} at ca. 70 K, and then dropped rapidly to 1.3×10^{-3} emu mol^{-1} upon cooling to 16 K. Below 16 K, an approximate plateau of χT was observed, which is consistent with the rapid increase in χ. The data above 130 K follows the Curie–Weiss law with C = 0.94 emu mol^{-1} K and θ = –62 K. These features suggest antiferromagnetic coupling between Cu^{II} ions, and the behavior below 16 K is attributable to the presence of a paramagnetic impurity.

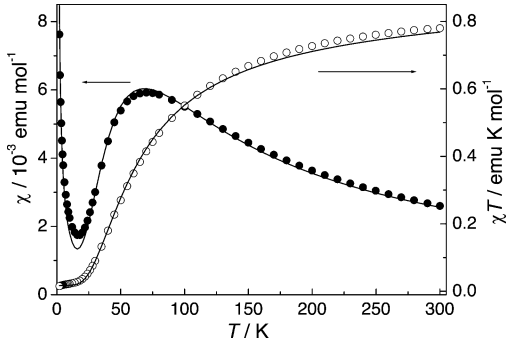

Figure 2. Thermal variations of χ and χT. The solid lines represent the best fit to the Bleaney–Bowers equation.

The experimental data were fitted with the modified Bleaney–Bowers equation[17] based on the Heisenberg Hamiltonian $\boldsymbol{H} = -J\boldsymbol{S}_1 \cdot \boldsymbol{S}_2$. The molar susceptibility per dimer is

$$\chi = \frac{2Ng^2\beta^2(1-\rho)}{kT[3+\exp(-J/kT)]} + \frac{Ng^2\beta^2\rho}{2kT} + N\alpha$$

where $N\alpha$ is the temperature-independent paramagnetism assumed to be 120×10^{-6} emu mol^{-1} per molecule, and ρ is the molar fraction of the paramagnetic impurity, which is assumed to be mononuclear Cu^{II} species. The impurity term is given for two Cu^{II} ions. The best fit leads to J = –78.6 cm^{-1}, g = 2.08, and ρ = 0.02, with $R = \Sigma(\chi_{obsd.} - \chi_{calcd.})^2/\Sigma\chi_{obsd.}^2 = 5.7 \times 10^{-4}$. The negative J value confirms a medium antiferromagnetic interaction in **1**.

In the previously reported binuclear Cu^{II} systems with double EO azido bridges, the magnetic interactions are usually ferromagnetic (J = 23–230 cm^{-1}) for symmetric eq–eq bridges[6,7] and may be weakly antiferromagnetic or ferromagnetic (J = –9–13 cm^{-1}) for asymmetric eq–ax bridges.[8,9] The medium antiferromagnetic interaction through the double eq–eq bridge in **1** is quite unusual and significantly stronger than those for eq–ax bridges. The interaction can be qualitatively interpreted as the result of two competing pathways. Whereas the N8 pathway with a small Cu–N–Cu angle (97.3°) is expected to transmit ferromagnetic exchange, the N5 pathway, which has a large Cu–N–Cu angle of 110.6°, should favor antiferromagnetic interactions as suggested by experimental studies on systems with mixed diazine and EO azido bridges[13] and previous theoretical calculations.[15] The observed antiferromagnetic interaction in **1** suggests that the ferromagnetic exchange through N8 is exceeded by the antiferromagnetic one through N5. With a magnetostructural goal in mind, the relative orientation of the magnetic orbitals controlled by the local distortion and asymmetric chelating ligand is likely to generate unusual magnetic properties. In order to analyze the interaction mechanism and to get more information on magnetostructural correlations, theoretical calculations were carried out on this intriguing system.

Theoretical Study

DFT calculations performed on **1**, **2**, and **3** are summarized in Table 2. The calculated magnetic constant in **1** is consistent with the experimental antiferromagnetic behavior. At this stage, the discrepancy with the measured amplitude is rather puzzling, though previous theoretical DFT studies have reported such inconsistency for Cu^{II} dimers.[18] As the N8 bridge angle value is set to the N5 one (110.6°, compound **2**), the antiferromagnetic character is significantly enhanced as J is reduced by 112 cm^{-1}. In contrast, **3** exhibits weak ferromagnetic character as anticipated by the reduction in the Cu–N5–Cu angle to 97.3°. These DFT results clearly suggest that a large Cu–N–Cu value favors antiferromagnetic interactions, in agreement with previous conclusions. Interestingly, one can conclude that the antiferromagnetic interaction through the Cu–N5–Cu pathway overtakes the ferromagnetic one mediated by the Cu–N8–Cu one. Nevertheless, (i) the apparent disagreement between the experimental and calculated exchange constant in **1** and (ii) the absence of relationship between the different J values calculated in compounds **1**, **2**, and **3** called for further inspections.

Table 2. Calculated exchange coupling constants J [cm^{-1}] in **1** and fictitious analogs **2** and **3** (for comparison, the experimental value for **1** is –78.6 cm^{-1}).

	DFT	CASSCF	DDCI-1	DDCI-3
1	–142	3	30	–104
2	–254	–14	–6	–218
3	22	13	60	21

Thus, complementary wavefunction-based calculations were carried out to grasp the origin of such fundamental differences. As a result of the size of the system, rather small basis sets were used. However, it was shown that the calculated exchange values do not greatly suffer from reduction

of the basis set, down to minimal ones.[19] Our results obtained by using different variational spaces following the DDCI methodology are summarized in Table 2.

Starting from the CAS[2,2]SCF triplet MOs (see Figure 3), the J values were estimated at the successive DDCI-1 and DDCI-3 levels of calculations. The magnetic orbitals display strong metallic character and correspond to the expected "e_g-like" singly occupied atomic orbitals (AOs) combinations. As a result of the local Jahn–Teller distortion around the Cu1 ion, the singly occupied AO involved is the $d_{x^2-y^2}$-type perpendicular to the axial Cu1–N2 bond, pointing towards the N3, N5, N8, and N14 atoms (see Figures 1 and 3). In contrast, the significant distortion of the Cu2 environment towards compressed trigonal bipyramidal results in a singly occupied d_{y^2}-type AO lying along the axial direction (N3–Cu2–N5) of the bipyramid. The MO pictures clearly illustrate that the symmetric N5 bridge should be a more efficient coupler than the asymmetric N8 one. As seen in Table 2, the exchange interactions are significantly influenced by the correlation effects introduced by the DDCI treatment. The antiferromagnetic character is indeed recovered at a DDCI-3 level of calculations in **1**, reaching reasonable agreement with experimental results. The antiferromagnetic behavior is greatly enhanced in fictitious compound **2**, as the value of $|J|$ is increased by approximately a factor of two. This is to be contrasted with our numerical estimate of the magnetic interaction in **3**, which turned out to be of weak ferromagnetic character.

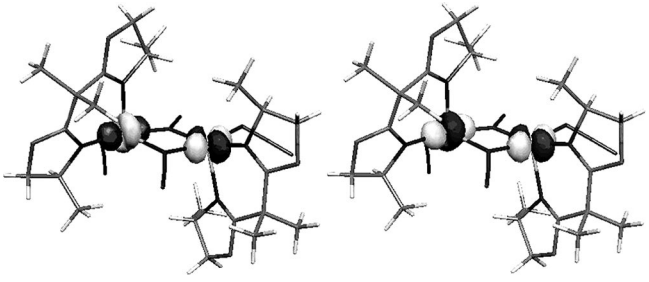

Figure 3. Active MOs resulting from a CAS[2,2]SCF calculation performed for the low-lying triplet state of **1**.

From our inspections performed upon double-bridge EO complex **1**, we can conclude that the exchange interaction is very sensitive to the Cu–N5–Cu angle. It is known from the literature[13] that the ferro/antiferro transition occurs at a critical value ca. 108° in such a compound. As observed in **2**, a slight deviation (less than 3°) from this value induces considerable antiferromagnetic character. Conversely, the occurrence of ferromagnetism is more progressive as the Cu–N8–Cu angle is reduced (see compound **3**). Therefore, one can effectively anticipate an antiferromagnetic behavior in **1**. Interestingly, the net exchange coupling constant in **1** is precisely the average between the corresponding DDCI values in **2** and **3**. Surprisingly, the DFT results do not offer such additive picture (see Table 2). Nevertheless, this particular observation can be understood by using the well-known Anderson's model,[20] as the superexchange interaction contributions are additive along the large Cu–N5–Cu and small Cu–N8–Cu pathways ($J = 2K - \frac{4t_{large}^2}{U} - \frac{4t_{small}^2}{U}$). Assuming that the latter are almost negligible ($t_{small} \approx 0$), the direct exchange K is $\approx 10\ cm^{-1}$ according to the calculated result of **3** (where the large-angle pathway is absent). Thus, assuming that the correlated characters controlled by the t_{eff}/U_{eff} factor are very similar, the effective hopping integral (t_{eff}) that governs the antiferromagnetic contributions between the two Cu^{II} ions is reduced in synthetic compound **1** relative to that of fictitious analog **2** by a factor of ca. 2, a rather spectacular effect for so small an angle modification.

Finally, a reading of the multireference wavefunction offers an interpretation of the underlying mechanisms. One may evaluate in the singlet state the relative weights of the so-called ionic and neutral forms. Let a and β be the valence MOs of the CAS[2,2]SCF triplet solution (see Figure 3). These MOs are mainly the in-phase and out-of-phase linear combinations of the d-type AOs a and b. Thus, the correlated singlet wavefunction $\lambda|a\bar{a}| - \mu|\beta\bar{\beta}|$ can be written in terms of the $|a\bar{a}|$, $|b\bar{b}|$ (two electrons localized on one copper center, i.e., ionic forms) and $|a\bar{b}|$, $|b\bar{a}|$ (neutral forms) determinants. The neutral and ionic weights in the wavefunction read $(\lambda - \mu)^2$ and $(\lambda + \mu)^2$, the ratio of which ρ defines the correlated character of the system. As a matter of fact, the larger the value of ρ, the higher the stabilization of the triplet state. As seen in Table 3, the correlated characters in **1** and **2** are almost identical, supporting our previous assumption that the t_{eff}/U_{eff} factors are very similar. Thus, the larger stabilization of the singlet state in **2** as compared to that of **1** confirms the enhancement in the effective hopping integral and should not be ascribed to a larger stabilization of the ionic forms. As expected from the ferromagnetic character of **3**, ρ decreases by almost a factor of 6 from DDCI-1 to DDCI-3. This result supports our previous assumption that the superexchange contributions in **3** were almost negligible. All our calculations performed upon the synthetic compound **1** and analogs **2** and **3** demonstrate the versatile character of the azido linker in the generation of molecular magnetic architectures.

Table 3. Values of $\rho(\times 10^{-2})$ [$\rho = (\lambda + \mu)^2/(\lambda - \mu)^2$] for complexes **1**, **2**, and **3**.

	CASSCF	DDCI-1	DDCI-3
1	43.9	5.9	2.7
2	22.4	10.0	2.6
3	286.5	50.0	8.3

Conclusion

In the present work, we have structurally and magnetically characterized an original binuclear Cu^{II}–azide complex involving a chiral bis(oxazoline) ligand. In the complex, the two Cu^{II} ions in distinct coordination geometries

are linked by two eq–eq end-on azido bridges. One bridge is quasisymmetric with short Cu–N distances, and the other is asymmetric with short and long Cu–N distances. Unprecedentedly, the two Cu–N–Cu bridging angles are, respectively, smaller and larger than the critical 108° value that distinguishes the ferromagnetic and antiferromagnetic regimes. These features are intriguing from the viewpoints of magnetostructural studies. It is observed from temperature-dependent magnetic susceptibility measurements that the two different bridges compete to settle a net antiferromagnetic coupling between the Cu^{II} ions. Complementary DFT and wavefunction-based calculations were performed to analyze the origin of such magnetic behavior. The importance of the bridging angles was quantified by varying this critical parameter. We showed that antiferromagnetism is very sensitive to the Cu–N–Cu angle that modulates the superexchange mechanism. Quantitatively, the magnetic interactions in **1** correspond to the average of the exchange constants in two fictitious structures with either two large or two small Cu–N–Cu angles. Thus, the control of the local transition-metal environments by the use of some specific chelating ligands allowed us to monitor the exchange coupling interactions through azido bridges.

Experimental Section

Materials and Measurements: All the starting chemicals were used as received. Elemental analyses (C, H, N) were performed with an Elementar Vario EL analyzer. IR spectra were recorded with a Nicolet Magna-IR 750 spectrometer equipped with a Nic-Plan Microscope. Temperature-dependent magnetic measurements were carried out with a Quantum Design SQUID MPMS-5 magnetometer with an applied field of 2 kOe, and the diamagnetic correction (-475×10^{-6} emu mol^{-1}) was made with Pascal's constants.

Synthesis of $[Cu_2(L)_2(N_3)_4]\cdot 0.5CH_3OH$ (1): A methanol solution (5 mL) of L (0.05 mmol, 17 mg) was added dropwise into a methanol solution (5 mL) of copper(II) acetate monohydrate (0.05 mmol, 10 mg). After stirring for 5 min, a methanol solution (5 mL) of sodium azide (0.1 mmol, 6.5 mg) was added with continuous stirring. Slow evaporation of the resulting solution at 4 °C in a refrigerator yielded dark-green crystals of **1**. Yield: 34.1%. The bulk phase purity of the sample was confirmed by powder X-ray diffraction. IR (KBr): $\tilde{\nu}$ = 2057 (s), 2034 (s), 1659 (m), 1475 (s), 1230 (s), 1123 (s), 701 (s) cm^{-1}. $C_{42.5}H_{46}Cu_2N_{16}O_{4.5}$ (980.03): calcd. C 52.09, H 4.73, N 22.87; found C 51.66, H 4.73, N 22.94.

Caution! Although not encountered in our experiments, metal complexes of azides are potentially explosive. Only a small amount of the materials should be prepared and handled with care.

Crystallographic Determination: Diffraction intensity data of the single crystal of **1** were collected at 298 K with a Bruker APEX II diffractometer equipped with a CCD area detector, equipped with graphite-monochromated Mo-K_α radiation (λ = 0.71073 Å). Empirical absorption corrections were applied by using the SADABS program.[21] All structures were solved by direct methods and refined by full-matrix least-squares analysis on F^2 with anisotropic thermal for all non-hydrogen atoms.[22] Hydrogen atoms in the complex molecule were placed at calculated positions and refined isotropically, and we were unable to locate the hydrogen atoms of the disordered lattice methanol molecule from the difference map. Crystal data: $C_{42.5}H_{46}Cu_2N_{16}O_{4.5}$, Mr = 980.03, Orthorhombic, space group $P2_12_12_1$, a = 15.0356(5) Å, b = 16.9982(6) Å, c = 18.4724(7) Å, V = 4721.1(3) Å^3, Z = 4, μ(Mo-K_α) = 0.961 mm^{-1}, $\rho_{calcd.}$ = 1.379 g cm^{-3}, T = 298 K, S = 1.048, R_1 = 0.0696 for 5022 reflections with $I > 2\sigma(I)$, and wR_2 = 0.1997 for 9244 independent reflections (R_{int} = 0.0788, 26879 collected reflections).

CCDC-668122 (for **1**) contains the supplementary crystallographic data for this paper. These data can be obtained free of charge from the Cambridge Crystallographic Data Centre via www.ccdc.cam.ac.uk/data_request/cif.

Computational Details: In order to grasp the origin of the magnetic coupling in the here-reported compound, quantum chemical calculations were performed. Our goal was to support the extracted coupling constant value and to investigate the sensitivity of this interaction upon the critical Cu–N–Cu angle values. Thus, DFT and wavefunction-based (ab initio configurations interactions, CI) calculations were used to probe the magnetic interactions. Whereas the former methodology allows one to investigate rather extended systems, it may suffer from the arbitrariness of the exchange correlation functional and may not always be appropriate. In contrast, CI calculations, which use the exact Hamiltonian, have proven to reach impressive agreement with experimental data.[4] In particular, the difference dedicated configurations interaction (DDCI) method[23] has been designed and applied to evaluate vertical energy differences, reaching spectroscopy accuracy.[4,24] The strength of wavefunction-based calculations is their ability to quantitatively distinguish the different underlying mechanisms (i.e., direct exchange, superexchange, spin polarization) contributing to the exchange coupling between the spin holder partners.[25] All our simulations were carried out by using the crystallographic data, comparing DFT and wavefunction-based approaches. Because the Cu^{II} ion exhibits a d^9 electronic configuration, the expected spin states result from the coupling between two s = 1/2 local spins, namely a singlet (S) and a triplet (T). By using the standard Heisenberg model Hamiltonian $\boldsymbol{H} = -J\boldsymbol{S}_1\cdot\boldsymbol{S}_2$, the exchange coupling constant reads $J = E_S - E_T$. DFT calculations were carried out by using the commonly accepted hybrid functional B3LYP.[26] with all electron TZVP basis sets for all the elements as implemented in the Gaussian 03 package.[27] Nevertheless, a single-determinant approach calls for the evaluation of a fictitious state energy (so-called broken-symmetry, BS).[28] Following the original development of Noodleman, the triplet-state energy E_T was initially converged to produce magnetic molecular orbitals (MOs) at an unrestricted level (i.e., UB3LYP). Then, the BS state was generated and the corresponding energy E_{BS} calculated through a standard self-consistent procedure. The exchange coupling constant was fully determined as a function of the triplet and BS energies difference and the magnetic orbitals overlap S_{ab}:

$$J = \Delta E_{ST} = (E_{BS} - E_T)/(1 + S_{ab}^2)$$

Since the through-space overlap is totally negligible considering the Cu–Cu distance (≈3.26 Å), J reduces to $E_{BS} - E_T$. Let us mention that the use of a not spin-projected formula leads to a similar expression for the coupling constant J.

In the meantime, we also performed explicitly correlated ab initio calculations that convey important information from a reading of the wavefunction. Thus, complete active space self-consistent field (CASSCF) calculations were first undertaken to generate a reference space including the leading electronic configurations in the desired spin multiplicities. The complete active space (CAS) should include at least the unpaired electrons on the different partners and the corresponding MOs. We restricted our inspections to the minimal active space (i.e., 2 electrons/2 MOs, CAS[2,2]). All these

preliminary CAS[2,2]SCF calculations were performed by using the Molcas 6.0 package,[29] with effective core potential for the Cu atoms with a (9s6p6d)/[3s3p4d] basis set contraction[30] and all electron basis sets for the rest of the elements (i.e., N,C,O (6s3p)/[2s1p] and H (3s)/[1s]).[31] It has been reported that a basis set enlargement from (4s3p2d) to (5s4p3d1f) upon the Cu atom and (2s1p) to (3s2p1d) on the N ones affects the calculated coupling constant by less than 11%.[19] The dynamical polarization and correlation effects were then incorporated by using the DDCI method as implemented in the CASDI code.[32] It has been clearly demonstrated that a bare valence-only description is not relevant to grasp such energy differences.[33] Thus, one should include selected configurations reached by excitations on top of the CASSCF wavefunction. As the number of degrees of freedom [i.e., holes in doubly occupied (inactive) MOs or particles generated in empty (virtual) MOs] grows, the successive DDCI-1, DDCI-2, and DDCI-3 levels are reached by expanding the CI space. Because the DDCI philosophy relies on the simultaneous characterization of different states that share similar spatial descriptions, one has to initially determine a set of common MOs to build up the CI space. Thus, the triplet-state CAS[2,2]SCF MOs were used to evaluate the singlet-triplet energy difference along the DDCI framework. Let us stress that the energetics are almost unaffected (less than 5%) by the use of the CASSCF singlet-state set of MOs.

Finally, considering the importance of the azido bridge characteristics, two fictitious analogs of **1** were built by varying the Cu–N–Cu angles. Model complexes **2** and **3** were constructed by making the two bridges strictly identical, whereas the Cu···Cu distance was maintained and unchanged. In complex **2**, both angles were set to the large angle value 110.6°, whereas in **3** these angles were 97.3°. By means of DFT and DDCI calculations performed upon such models, our goal was to provide an interpretation of the exchange interaction by splitting the contributions along the large- and small-angle pathways in synthetic compound **1**.

Supporting Information (see footnote on the first page of this article): Figure showing the weak intermolecular hydrogen bonds in **1**.

Acknowledgments

We are thankful for the financial support from the Natural Science Foundation of China (Nos. 20571026 and 20771038) and the Ministry of Education of China (NCET-05-0425). The "Institut du Développement et des Ressources en Informatique Scientifique" (IDRIS) is acknowledged for computing facilities.

[1] a) O. Kahn, *Molecular Magnetism*, VCH, New York, **1993**; b) J. S. Miller, *Adv. Mater.* **2002**, *14*, 1105–1109; c) J. S. Miller, M. Drillon (Eds.), *Magnetism: Molecules to Materials*, Wiley-VCH, Weinheim, **2002**–**2005**, vols. I–V.

[2] Reviews: a) J. Ribas, A. Escuer, M. Monfort, R. Vicente, R. Cortés, L. Lezama, T. Rojo, *Coord. Chem. Rev.* **1999**, *193–195*, 1027–1068; b) A. Escuer, G. Aromi, *Eur. J. Inorg. Chem.* **2006**, 4721–4736; c) X.-Y. Wang, Z.-M. Wang, S. Gao, *Chem. Commun.* **2008**, 281–294.

[3] Recent examples: a) X.-T. Liu, X.-Y. Wang, W.-X. Zhang, P. Cui, S. Gao, *Adv. Mater.* **2006**, *18*, 2852–2856; b) Y.-F. Zeng, J.-P. Zhao, B.-W. Hu, X. Hu, F.-C. Liu, J. Ribas, J. Ribas-Ariño, X.-H. Bu, *Chem. Eur. J.* **2007**, *13*, 9924–9930; c) Y. S. You, J. H. Yoon, H. C. Kim, C. S. Hong, *Chem. Commun.* **2005**, *32*, 4116–4118; d) A. Escuer, F. A. Mautner, M. A. S. Goher, M. A. M. Abu-Youssef, R. Vicente, *Chem. Commun.* **2005**, *5*, 605–607; e) X.-Y. Wang, L. Wang, Z.-M. Wang, S. Gao, *J. Am. Chem. Soc.* **2006**, *128*, 674–675; f) X.-Y. Wang, Z.-M. Wang, S. Gao, *Inorg. Chem.* **2008**, *47*, 5720–5724; g) B. Bitschnau, A. Egger, A. Escuer, F. A. Mautner, B. Sodin, R. Vicente, *Inorg. Chem.* **2006**, *45*, 868–876.

[4] a) M. A. Carvajal, C. Aronica, D. Luneau, V. Robert, *Eur. J. Inorg. Chem.* **2007**, *28*, 4434–4437; b) C. Aronica, E. Jeanneau, H. El Moll, D. Luneau, B. Gillon, A. Goujon, A. Cousson, M. A. Carvajal, V. Robert, *Chem. Eur. J.* **2007**, *13*, 3666–3674; c) M. L. Bonnet, C. Aronica, G. Chastanet, G. Pilet, D. Luneau, C. Mathonière, R. Clérac, V. Robert, *Inorg. Chem.* **2008**, *47*, 1127–1130.

[5] a) E.-Q. Gao, S.-Q. Bai, Z.-M. Wang, C.-H. Yan, *J. Am. Chem. Soc.* **2003**, *125*, 4984–4985; b) E.-Q. Gao, Z.-M. Wang, C.-H. Yan, *Chem. Commun.* **2003**, 1748–1749; c) E.-Q. Gao, S.-Q. Bai, Y.-F. Yue, Z.-M. Wang, C.-H. Yan, *Inorg. Chem.* **2003**, *42*, 3642–3649; d) E.-Q. Gao, Y.-F. Yue, S.-Q. Bai, Z. He, C.-H. Yan, *Chem. Mater.* **2004**, *16*, 1590–1594; e) E.-Q. Gao, Y.-F. Yue, S.-Q. Bai, Z. He, C.-H. Yan, *J. Am. Chem. Soc.* **2004**, *126*, 1419–1429; f) E.-Q. Gao, A.-L. Cheng, Y.-X. Xu, M.-Y. He, C.-H. Yan, *Inorg. Chem.* **2005**, *44*, 8822–8835; g) P.-P. Liu, A.-L. Cheng, N. Liu, W.-W. Sun, E.-Q. Gao, *Chem. Mater.* **2007**, *19*, 2724–2726; h) E.-Q. Gao, P.-P. Liu, Y.-Q. Wang, Q. Yue, Q.-L. Wang, *Chem. Eur. J.* **2009**, *15*, 1217–1226.

[6] a) J. Comarmond, P. Plumere, J. M. Lehn, Y. Agnus, R. Louis, R. Weiss, O. Kahn, I. Morgenstern-Badarau, *J. Am. Chem. Soc.* **1982**, *104*, 6330–6347; b) O. Kahn, S. Sicorav, J. Gouteron, S. Jeannin, Y. Jeannin, *Inorg. Chem.* **1983**, *22*, 2877–2883; c) S. Sikorav, I. Bkouche-Waksman, O. Kahn, *Inorg. Chem.* **1984**, *23*, 490–495; d) B. Graham, M. T. W. Hearn, P. C. Junk, M. Kepert, F. E. Mabbs, B. Moubaraki, K. S. Murray, L. Spiccia, *Inorg. Chem.* **2001**, *40*, 1536–1543.

[7] a) S. Youngme, T. Chotkhun, S. Leelasubcharoen, N. Chaichit, C. Pakawatchai, G. A. van Albada, J. Reedijk, *Polyhedron* **2007**, *26*, 725–735; b) A. Escuer, M. A. S. Goher, F. A. Mautner, R. Vicente, *Inorg. Chem.* **2000**, *39*, 2107–2112; c) G. A. van Albada, J. T. Lakin, N. Veldman, A. L. Spek, J. Reedijk, *Inorg. Chem.* **1995**, *34*, 4910–4917.

[8] a) M. S. Ray, A. Ghosh, R. Bhattacharya, G. Mukhopadhyay, M. G. B. Drew, J. Ribas, *Dalton Trans.* **2004**, 252–259; b) P. Manikandan, R. Muthukumaran, K. R. J. Thomas, B. Varghese, G. V. R. Chandramouli, P. T. Manoharan, *Inorg. Chem.* **2001**, *40*, 2378–2389; c) S. Koner, S. Saha, T. Mallah, K. I. Okamoto, *Inorg. Chem.* **2004**, *43*, 840–842; d) A. Escuer, M. Font-Bardia, S. S. Massoud, F. A. Mautner, E. Penalba, X. Solans, R. Vicente, *New J. Chem.* **2004**, *28*, 681–686.

[9] a) M. S. Ray, A. Ghosh, S. Chaudhuri, M. G. B. Drew, J. Ribas, *Eur. J. Inorg. Chem.* **2004**, 3110–3117; b) R. Cortés, M. K. Urtiaga, L. Lezama, J. I. R. Larramendi, M. I. Arriortua, T. Rojo, *J. Chem. Soc., Dalton Trans.* **1993**, 3685–3694; c) S.-Q. Bai, E.-Q. Gao, Z. He, C.-J. Fang, C.-H. Yan, *New J. Chem.* **2005**, *29*, 935–941.

[10] a) P. Chaudhuri, K. Oder, K. Wieghardt, B. Nuber, J. Weis, *Inorg. Chem.* **1986**, *25*, 2818–2824; b) Y. Agnus, R. Louis, J. P. Gisselbrecht, R. Weiss, *J. Am. Chem. Soc.* **1984**, *106*, 93–102.

[11] a) T. R. Felthouse, D. N. Hendrickson, *Inorg. Chem.* **1978**, *17*, 444–456; b) I. Bkouche-Waksman, S. Sikorav, O. Kahn, *J. Crystallogr. Spectrosc. Res.* **1983**, *13*, 303–310; c) A. Escuer, M. Font-Bardia, E. Penalba, X. Solans, R. Vicente, *Inorg. Chim. Acta* **2000**, *298*, 195–201; d) Y. Xie, Q. Liu, H. Jiang, C. Du, X. Xu, M. Yu, Y. Zhu, *New J. Chem.* **2002**, *26*, 176–179.

[12] a) M. F. Charlot, O. Kahn, M. Chaillet, C. Larrieu, *J. Am. Chem. Soc.* **1986**, *108*, 2574–2581; b) I. von Seggern, F. Tuczek, W. Bensch, *Inorg. Chem.* **1995**, *34*, 5530–5547; c) C. Blanchet-Boiteux, J. M. Mouesca, *J. Am. Chem. Soc.* **2000**, *122*, 861–869.

[13] a) S. S. Tandon, L. K. Thompson, M. E. Manuel, J. N. Bridson, *Inorg. Chem.* **1994**, *33*, 5555–5570; b) L. K. Thompson, S. S. Tandon, M. E. Manuel, *Inorg. Chem.* **1995**, *34*, 2356–2366.

[14] M. A. Aebersold, B. Gillon, O. Plantevin, L. Pardi, O. Kahn, P. Bergerat, I. von Seggern, F. Tuczek, L. Öhrström, A. Grand, E. Lelièvre-Berna, *J. Am. Chem. Soc.* **1998**, *120*, 5238–5245.

[15] a) E. Ruiz, J. Cano, S. Alvarez, P. Alemany, *J. Am. Chem. Soc.* **1998**, *120*, 11122–11129; b) C. Adamo, V. Barone, A. Bencini, F. Totti, I. Ciofini, *Inorg. Chem.* **1999**, *38*, 1996–2004.
[16] W. Addison, T. N. Rao, J. Reedijk, J. van Rijn, G. C. Verschoor, *J. Chem. Soc., Dalton Trans.* **1984**, 1349–1356.
[17] B. Bleaney, K. D. Bowers, *Proc. R. Soc. London, Ser. A* **1952**, *214*, 451–459.
[18] C. Desplanches, E. Ruiz, A. Rodriguez-Fortea, S. Alvarez, *J. Am. Chem. Soc.* **2002**, *124*, 5197–5205.
[19] J. Cabrero, C. de Graaf, E. Bordas, R. Caballol, J. P. Malrieu, *Chem. Eur. J.* **2003**, *9*, 2307–2315.
[20] a) P. W. Anderson, *Phys. Rev.* **1950**, *79*, 350–356; b) P. W. Anderson in *Theory of the Magnetic Interaction: Exchange in Insulators and Superconductors* (Eds.: F. Turnball, F. Seitz), Academic Press, New York, **1963**, vol. 14, p. 99.
[21] G. M. Sheldrick, *Program for Empirical Absorption Correction of Area Detector Data*, University of Göttingen, Germany, **1996**.
[22] G. M. Sheldrick, *SHELXTL*, Version 5.1, Bruker Analytical X-ray Instruments, Inc., Madison, Wisconsin, USA, **1998**.
[23] J. Miralles, O. Castell, R. Caballol, J. P. Malrieu, *Chem. Phys.* **1993**, *172*, 33–43.
[24] a) J. Cabero, N. Ben Amor, C. de Graaf, F. Illas, R. Calaboll, *J. Phys. Chem. A* **2000**, *104*, 9983–9989; b) R. Bastardis, C. de Graaf, N. Guihéry, *Phys. Rev. B* **2008**, *77*, 054426; c) S. Zein, F. Neese, *J. Phys. Chem. A* **2008**, *112*, 7976–7983.
[25] a) J. C. Calzado, J. Cabrero, J. P. Malrieu, R. Caballol, *J. Chem. Phys.* **2002**, *116*, 2728–2746; b) J. C. Calzado, J. Cabrero, J. P. Malrieu, R. Caballol, *J. Chem. Phys.* **2002**, *116*, 3985–4000.
[26] a) A. D. Becke, *Phys. Rev. A* **1988**, *38*, 3098–3100; b) A. D. Becke, *J. Chem. Phys.* **1993**, *98*, 5648–5652.
[27] M. J. Frisch, G. W. Trucks, H. B. Schlegel, G. E. Scuseria, M. A. Robb, J. R. Cheeseman, J. A. Montgomery Jr, T. Vreven, K. N. Kudin, J. C. Burant, J. M. Millam, S. S. Iyengar, J. Tomasi, V. Barone, B. Mennucci, M. Cossi, G. Scalmani, N. Rega, G. A. Petersson, H. Nakatsuji, M. Hada, M. Ehara, K. Toyota, R. Fukuda, J. Hasegawa, M. Ishida, T. Nakajima, Y. Honda, O. Kitao, H. Nakai, M. Klene, X. Li, J. E. Knox, H. P. Hratchian, J. B. Cross, V. Bakken, C. Adamo, J. Jaramillo, R. Gomperts, R. E. Stratmann, O. Yazyev, A. J. Austin, R. Cammi, C. Pomelli, J. W. Ochterski, P. Y. Ayala, K. Morokuma, G. A. Voth, P. Salvador, J. J. Dannenberg, V. G. Zakrzewski, S. Dapprich, A. D. Daniels, M. C. Strain, O. Farkas, D. K. Malick, A. D. Rabuck, K. Raghavachari, J. B. Foresman, J. V. Ortiz, Q. Cui, A. G. Baboul, S. Clifford, J. Cioslowski, B. B. Stefanov, G. Liu, A. Liashenko, P. Piskorz, I. Komaromi, R. L. Martin, D. J. Fox, T. Keith, M. A. Al-Laham, C. Y. Peng, A. Nanayakkara, M. Challacombe, P. M. W. Gill, B. Johnson, W. Chen, M. W. Wong, C. Gonzalez, J. A. Pople, *Gaussian 03*, Revision C. 02, Gaussian, Inc., Wallingford, CT, **2004**, p. 214.
[28] a) L. Noodleman, J. G. Norman Jr, *J. Chem. Phys.* **1979**, *70*, 4903–4906; b) L. Noodleman, *J. Chem. Phys.* **1981**, *74*, 5737–5743; c) L. Noodleman, E. R. Davidson, *Chem. Phys.* **1986**, *109*, 131–143; d) L. Noodleman, C.-Y. Peng, D. A. Case, J. M. Mouesca, *Coord. Chem. Rev.* **1995**, *144*, 199–244.
[29] G. Karlström, R. Lindh, P. A. Malmqvist, B. O. Roos, U. Ryde, V. Veryazov, P. O. Widmark, M. Cossi, B. Schimmelpfennig, P. Neogrady, L. Seijo, *Comput. Mater. Sci.* **2003**, *28*, 222–239.
[30] Z. Barandiarán, L. Seijo, *Can. J. Chem.* **1992**, *70*, 409–415.
[31] W. J. Hehre, R. F. Stewart, J. A. Pople, *J. Chem. Phys.* **1969**, *51*, 2657–2664.
[32] N. Ben Amor, D. Maynau, *Chem. Phys. Lett.* **1998**, *286*, 211–220.
[33] J. B. Rota, L. Norel, C. Train, N. Ben Amor, D. Maynau, V. Robert, *J. Am. Chem. Soc.* **2008**, *130*, 10380–10385.

Received: March 3, 2009
Published Online: May 28, 2009

